Current Applied Science and Technology e-ISSN: 2586-9396

Curr. Appl. Sci. Technol. 2026, Vol. 26 (No.5), e0268155

Research article

Effects of Sputtering Power and Gamma Radiation Dose on the Optical and Electrical Properties of ITO Films

Nalutporn Phiboon[1], Watcharaporn Thongjoon[1], Chantana Aiempanakit[2], Akapong Phunpueok[2], Sarawut Jaiyen[2], Montri Aiempanakit[3] and Kamon Aiempanakit[1]*

[1]Department of Physics, Faculty of Science and Technology, Thammasat University, Pathumthani 12121, Thailand
[2]Division of Physics, Faculty of Science and Technology, Rajamangala University of Technology Thanyaburi, Pathumthani 12110, Thailand
[3]Department of Physics, Faculty of Science, Silpakorn University Nakhon Pathom 73000, Thailand

Received: 25 June 2025, Revised: 18 August 2025, Accepted: 15 September 2025, Published: 16 January 2026

Abstract

ITO films were deposited on glass substrates using DC magnetron sputtering at different sputtering powers of 10 and 20 W. All films were irradiated with gamma radiation at doses ranging from 0 to 150 kGy. XRD results showed that ITO films at 10 W sputtering power exhibited decreased crystallinity with increasing gamma doses, while films at 20 W showed higher crystallinity at 50 kGy, which then decreased with further irradiation. The optical transmittance and energy band gap decreased with increasing doses, indicating structural changes due to defect formation. The electrical resistivity of the ITO film increased with the irradiated dose for a sputtering power of 10 and 20 W due to the increased defect formation in the structure. Even though the sputtering power condition was 20 W, after irradiation with a dose of 50 kGy, the ITO film exhibited higher crystallinity but had a predominant change in the (222) plane instead of the (400) plane. This study revealed the important role of deposition parameters and gamma irradiation in controlling structural, optical, and electrical properties of ITO films. The reduced resulting energy band gap is linked to increased resistance in ITO films after exposure to gamma radiation, with defect formation.

Keywords: gamma radiation; indium tin oxide; sputtering; morphology; optical and electrical properties

1. Introduction

Thin film technology has rapidly advanced in recent years, revolutionizing various industrial applications and manufacturing processes. These thin films are widely utilized in numerous industrial products, including coatings for eyeglass lenses, building glass, and automotive window films, due to their enhanced resistance to chemicals and abrasion. Additionally,

*Corresponding author: E-mail: kamon.aie@hotmail.com
https://doi.org/10.55003/cast.2026.268155
Copyright © 2026 by King Mongkut's Institute of Technology Ladkrabang, Thailand. This is an open access article under the CC BY-NC-ND license (http://creativecommons.org/licenses/by-nc-nd/4.0/).

thin films are integral components in advanced device such as flat-panel displays, organic light-emitting diodes (OLEDs) (Coutts et al., 2000), gas sensors (Al-Hardan et al., 2013; Comini et al., 2013), photovoltaics, and optoelectronic devices.

The desirable properties for conducting oxide films currently include (1) low specific resistivity, (2) good thermal stability, (3) good homogeneity across the substrate, (4) low particle contamination, (5) good adhesion to the substrate, and (6) low manufacturing costs (Maknys et al., 2006; Khodorov et al., 2007; Venkatachalam et al., 2011; Mustapha et al., 2013; Mustapha et al., 2018). A widely used material is indium tin oxide (ITO), an n-type semiconductor. It is among the most extensively employed thin films owing to its exceptional electrical conductivity, high optical transmittance in the visible range, and reflective properties in the infrared region. These characteristics make ITO an essential material in applications ranging from energy-saving window coatings to optoelectronic devices, such as liquid crystal displays (LCDs), plasma screens, and touch panels. Various techniques have been developed to prepare ITO films, including radio frequency (RF) magnetron sputtering, reactive RF sputtering (Wu et al., 1996; Wohlmuth & Adesida., 2005), pulsed laser deposition (PLD) (Yan et al., 2001), dip coating (Tahar et al., 2001), sol-gel methods (Diliegros-Godines et al., 2014), and chemical vapor deposition (CVD) (Li et al., 2004).

Exposure to gamma radiation alters the properties of thin films by inducing changes in crystal structure (Kumaravel et al., 2010) and generating defects that influence material performance (El-Nahass et al., 2009; 2010; Oryema et al., 2020). These modifications significantly influence their electrical conductivity, optical transmittance, and other material properties. Previous studies, such as those by Kajal et al. (2023), demonstrated that SnO_2 films irradiated with gamma rays exhibited increased crystallite size, decreased energy bandgap, and improved electrical conductivity. Similarly, Al-Baradi et al. (2014) reported that gamma-irradiated Cd_2SnO_4 films showed a reduction in energy bandgap and refractive index, highlighting the influence of radiation on carrier distribution and defect density.

However, relatively few studies have focused on gamma irradiation effects in ITO films prepared via DC magnetron sputtering, particularly under non-annealed conditions where the film structure remains partially disordered. In practical applications such as flexible electronics, radiation-hardened sensors, and spaceborne systems, post-deposition annealing may not be feasible due to temperature constraints or in situ fabrication requirements (Kulkarni et al., 1997; Chauhan et al., 2014; Kim et al., 2015). In these environments, ITO films often exhibit lower crystallinity and higher defect densities, making their radiation response behavior especially relevant.

In addition, although our films are not annealed, we intentionally deposited them on glass substrates rather than polymers. This choice allows direct comparison with previous studies on ITO-on-glass systems that have been evaluated under gamma irradiation, including the work of Alyamani and Mustapha (2016), where ITO films prepared by PLD on glass demonstrated good retention of optical and electrical performance even after exposure to high gamma doses. By keeping the substrate type constant, we aim to isolate the effects of irradiation on film structure while enabling meaningful future comparison with annealed or commercial ITO coatings.

To address this gap, this study investigates the combined influence of sputtering power and gamma irradiation on the structural, optical, and electrical properties of ITO thin films deposited at room temperature without annealing. This approach provides insight into the radiation response of disordered ITO films, aiming to support the design of transparent conductive materials suitable for use in low-temperature or radiation-intensive applications.

2. Materials and Methods

2.1 Experimental details

ITO thin films were deposited onto glass slides using the direct current (DC) magnetron sputtering method at room temperature. The target material used for deposition was ITO (purity 99.999%, 2-inch diameter, 0.25-inch thickness; Kurt J. Lesker). Glass slides (1 × 3 inches) served as substrates and were ultrasonically cleaned in deionized water, acetone, and 2-propanol for 15 min each, followed by air drying. The substrate-to-target distance was maintained at approximately 80 mm throughout the deposition process. The diagram of the DC magnetron sputtering system is shown in Figure 1.

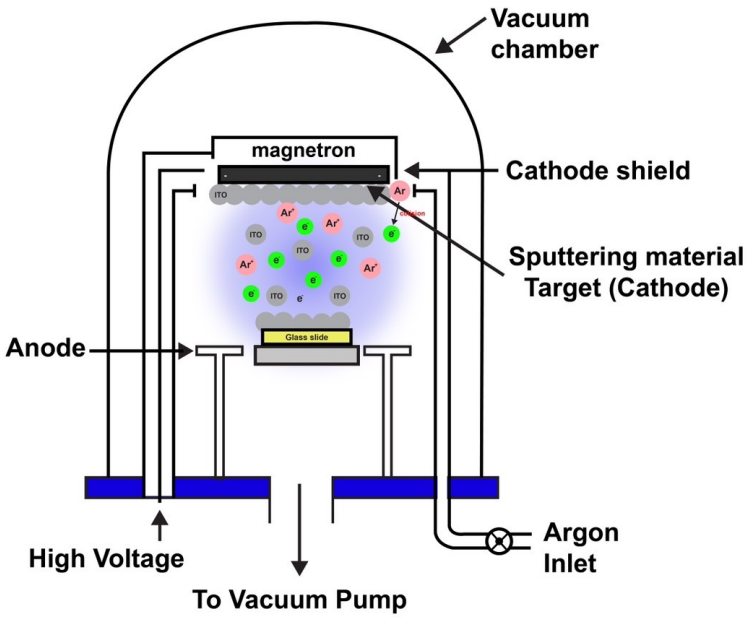

Figure 1. DC magnetron sputtering system for deposition of ITO films

The sputtering chamber was evacuated to a base pressure of 5×10^{-5} mTorr using a combination of diffusion and rotary pumps. High-purity argon gas (99.9999% purity) was introduced at a flow rate of 15 sccm to sustain the sputtering plasma. Pre-sputtering was performed for 5 min to remove surface oxides on the target to ensure a clean surface. During deposition, the sputtering power was set to 10 and 20 W, producing ITO films with thicknesses of 200 nm.

After deposition, the samples were irradiated with gamma rays at doses of 0, 50, 100, and 150 kGy. The irradiation was carried out in a non-temperature-controlled environment, with ambient temperatures estimated between 25°C and 30°C. However, the actual sample temperature during exposure may have been higher due to the thermal properties and geometry of the material. The gamma dose rate was approximately 3 kGy/h. generated by an irradiation system manufactured by Paul Stephens Consultancy Ltd., United Kingdom.

2.2 Analysis techniques

The films were characterized using multiple techniques. X-ray diffraction (XRD) analysis was performed with Cu Kα radiation (λ = 1.5406 Å) over a 2θ range of 20° to 80° using a Bruker D2 PHASER to determine the crystal structure. Surface morphology was observed using a field-emission scanning electron microscope (FE-SEM; TESCAN MIRA-3, Czech Republic). Optical properties, including transmittance and energy bandgap, were measured using a UV-Vis spectrophotometer (UV 800 Spectrophotometer). Electrical properties were evaluated using the four-point probe method (ECOPIA, HMS-3000).

2.3 Statistical analysis

All measurements were performed in triplicate, and the results were reported as mean values ±standard error. Data processing, including calculation of statistical parameters and determination of intercept points from plots (e.g., bandgap estimation), was performed using Microsoft Excel and Origin 2019b software. No further statistical hypothesis testing was conducted.

3. Results and Discussion

3.1 X-ray diffraction studies

The crystal structure of the ITO films before and after gamma irradiation was analyzed using XRD, as shown in Figure 2. The results showed that the ITO films maintained distinct crystal structures under all conditions. The XRD peaks corresponding to the (222) and (400) planes were observed at 2θ values of 30.56° and 35.23°, respectively, indicating a body-centered cubic (bcc) structure consistent with JCPDS No. 89-4595. For the unirradiated ITO films, crystallization was mainly observed along the (400) plane, with the peak intensity influenced by the sputtering power and oxide formation, as reported in previous studies (Rossnagel, 2001; Aiempanakit et al., 2009).

Considering the effect of sputtering power, ITO films deposited at 20 W generally exhibited higher initial crystallinity and stronger (400) orientation compared to those deposited at 10 W, which showed weaker crystallinity and smaller crystallite size.

With respect to gamma irradiation dose, lower doses (50 kGy) induced partial recrystallization and promoted the (222) orientation, whereas higher doses (100-150 kGy) introduced structural disorder, reduced peak intensity, and increased microstrain, particularly in films deposited at 20 W.

Gamma irradiation affects the crystal structure as it causes the formation of defects, such as vacancies and interstitials, which are caused by the ejection of atoms in the film from their original positions, causing damage and reducing the integrity of the crystal structure. The accumulation of these defects decreases the peak intensity at the (400) plane and results in a distorted atomic arrangement. This change is evident from the films irradiated at 100 kGy and 150 kGy, where increasing the irradiation dose caused more defects and decreased the crystallinity in the (400) plane peak. However, the films irradiated at 50 kGy showed a significant increase in crystallinity along the (222) plane. In contrast, increasing the gamma irradiation dose to 100 and 150 kGy resulted in a significant decrease in the crystallinity, especially in the films deposited at 20 W. This decrease is due to structural damage and defect formation, which is consistent with the findings of Kajal et

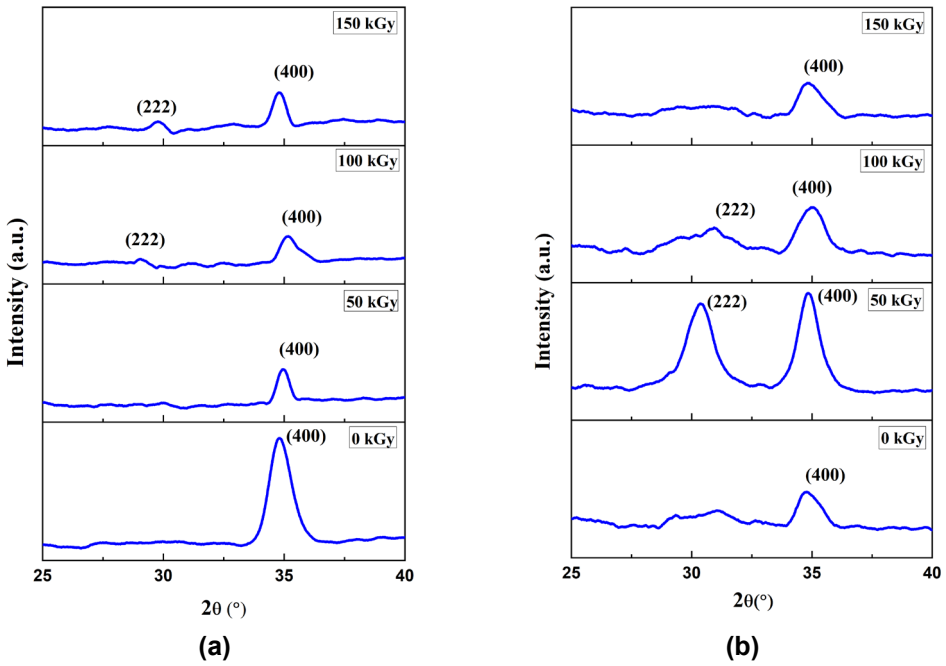

Figure 2. X-ray diffraction peaks of ITO films prepared with sputtering powers of (a) 10 and (b) 20 W after gamma radiation at doses of 0, 50, 100, and 150 kGy.

al. (2023). For the films deposited at 10 W, the intensity of the (400) plane decreased with increasing gamma irradiation dose, while the intensity of the (222) plane increased at 100 and 150 kGy. The changes suggest that gamma irradiation affects the preferred crystallographic orientation, depending on the deposition power and the irradiation dose. The observed structural changes in the XRD patterns were analyzed using Bragg's law, which relates the diffraction angle to the interplanar spacing, and the lattice parameter equation. Additionally, the crystallite size (D) and microstrain (ε) of both the pure and gamma-irradiated ITO films were determined using the Scherrer equation (equation 1) and the Williamson-Hall method (equation 2) (Aldawood & Ali, 2024). These calculated values are presented in Table 1.

$$D = \frac{k\lambda}{\beta\cos\theta} \tag{1}$$

Here, D is crystallite size (nm), k = 0.9 is the constant shape factor, β is full-width half maxima (radians), λ is the X-ray wavelength used (λ = 1.540 Å) and θ is the diffraction angle.

$$\beta\cos\theta = \frac{k\lambda}{D} + 4\varepsilon\sin\theta \tag{2}$$

where ε is the micro strain. Other terms are the same as above.

In summary, sputtering power determined the initial degree of crystallinity, while gamma irradiation dose controlled the extent of recrystallization or defect generation, leading to orientation changes between the (400) and (222) planes.

ITO films produced with a power of 10 W showed a continuous decrease in both the lattice parameter and d-spacing when exposed to gamma radiation at 50 and 100 kGy, followed by an increase at 150 kGy. Similarly, for the films deposited at 20 W, the lattice parameter and d-spacing decreased at 50 kGy and increased at 100 and 150 kGy. Moreover, the crystallite size of the ITO films also tended to change. The various values are shown in Table 1.

Table 1. The calculated values of structural parameters of ITO films before and after irradiation at different doses

Sample	Gamma Dose (kGy)	d_{hkl} (Å)	a (nm)	D (nm)	ε ($x10^{-2}$)
10 W	0	2.57341	1.02936	7.62	1.51
	50	2.56332	1.02533	12.42	0.92
	100	2.54765	1.01906	7.64	1.50
	150	2.57486	1.02994	11.09	1.10
20 W	0	2.57341	1.02936	6.68	1.73
	50	2.55761	1.02304	7.82	1.48
	100	2.57196	1.02879	6.62	1.73
	150	2.57341	1.02936	6.93	1.68

3.2 Structural and morphological analysis

Figure 3 presents top-view and cross-sectional SEM images used to investigate the structure and morphology of ITO thin films on glass substrates under varying irradiation intensities. The influence of sputtering power is evident: relative to 10 W, films deposited at 20 W exhibited denser microstructures and larger grain agglomerates. The study found that ITO films deposited at powers of 10 and 20 W without irradiation exhibited rough and uneven surfaces, indicating structural imperfections. However, the films remained intact without any delamination. As for the effect of gamma irradiation dose, the surface morphology progressively changed with increasing dose, from smoother grains at 50 kGy to fragmented grains and defect-related roughness at 100-150 kGy. Upon irradiation at 50 kGy, the surfaces became smoother, consistent with partial structural alignment, and this was accompanied by more pronounced grain agglomeration at 20 W, in line with the higher crystallinity observed at this condition. As the irradiation intensity increased to 100 kGy, the surface of ITO films began to break into small grains distributed throughout the samples. These changes were consistent with the behavior of ITO films under irradiation, where the increased atomic displacement within the crystal lattice induces structural defects that lead to film deterioration. The surface morphology of ITO films reflected the structural changes occurring in the ITO layer. At an irradiation intensity of 150 kGy, the surface of the ITO film

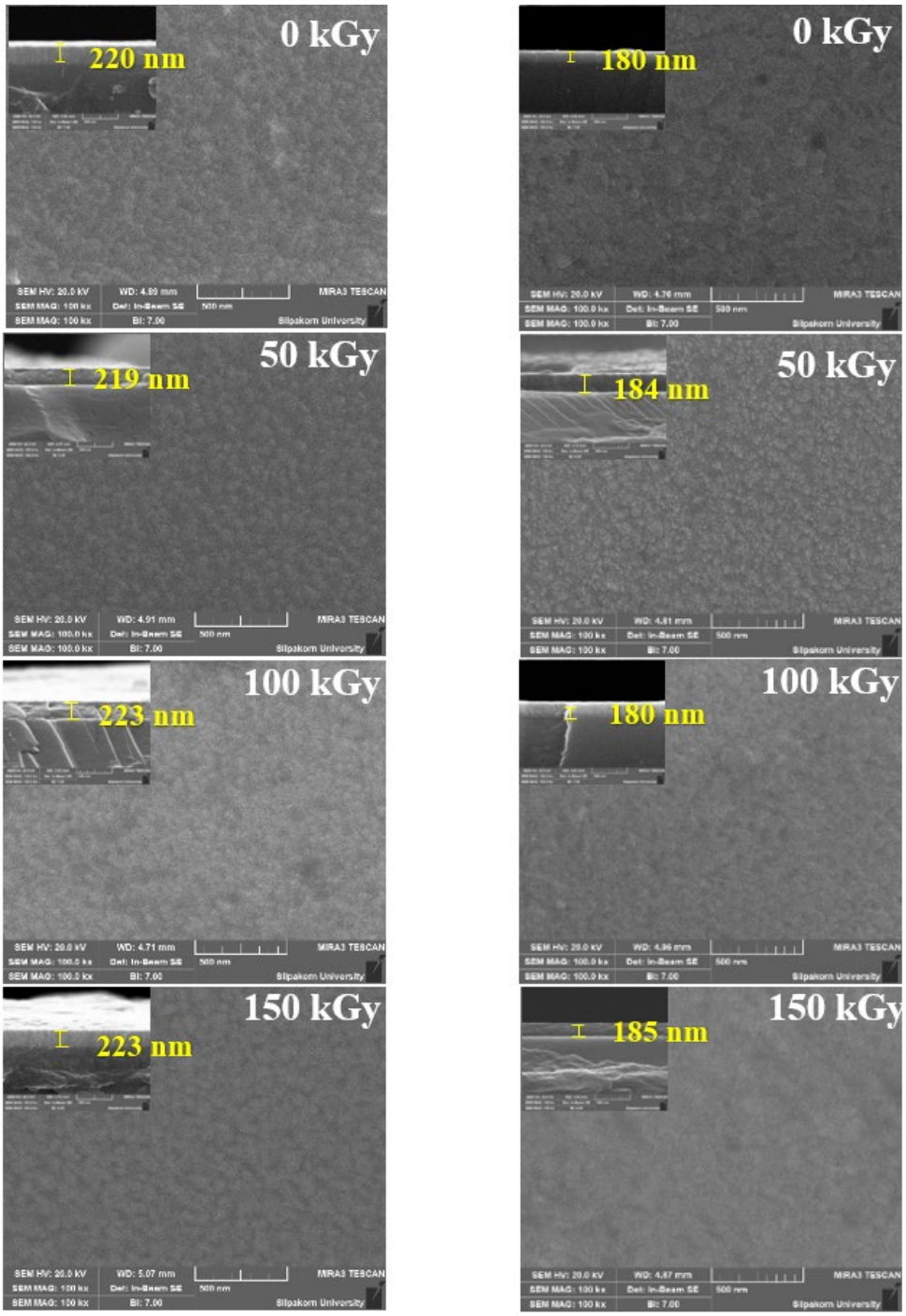

Figure 3. FE-SEM images showing the morphological characteristics of ITO films irradiated with gamma radiation at various dose levels.

at a sputtering power of 10 W appeared to have more pronounced grain formation than at the 20 W condition. These changes were due to important radiation-induced defects in the ITO film, which may lead to partial atomic rearrangement and surface restructuring, as well as the effect of oxygen in the film and the atmosphere. Additionally, irradiation caused oxygen loss from the ITO structure, producing oxygen vacancies within the lattice.

The elemental composition of ITO films was analyzed using energy-dispersive X-ray spectroscopy (EDS) to examine the effects of gamma irradiation on chemical stability. Figure 4 presents the EDS spectra of ITO films deposited at 10 W and 20 W under different irradiation doses. The analysis confirmed the consistent presence of indium (In), tin (Sn), and oxygen (O) in all samples, with no contamination detected. Especially at a power of 10 W, the oxygen content remained relatively stable across all radiation doses, indicating that gamma irradiation did not significantly deplete oxygen from the ITO lattice. This suggests that the structural degradation observed in FE-SEM images (e.g., grain formation or decay) was due to atoms being excited and changing their structural arrangement during radiation rather than oxygen loss. This rearrangement during gamma irradiation was likely attributed to the high-energy radiation providing sufficient energy to the crystal lattice, enabling atomic displacement and reorganization, leading directly to the generation of structural defects within the film. EDS analysis indicates a more stable oxygen stoichiometry in the 10 W film, implying enhanced chemical resistance to gamma radiation compared to the 20 W counterpart. These findings demonstrate that the overall stoichiometry of ITO films remained stable even after high-dose irradiation. In the case of 20 W power, the oxygen content was higher than in the 10 W power condition. The elemental composition ratio was not constant at 50 kGy irradiation and constant at 100 and 150 kGy. This variation showed that at a power of 20 W, the elemental composition of the films varied with the exposure dose. The films tended toward equilibrium at the high doses of 100 and 150 kGy. However, the occurrence of local defects and microstructural changes may still affect the electrical and optical properties of the films.

In summary, higher sputtering power (20 W) generally enhanced crystallinity and grain agglomeration, whereas lower power (10 W) films were more susceptible to high-dose irradiation. Low to moderate doses can improve surface morphology, while high doses induce defect-dominated roughening.

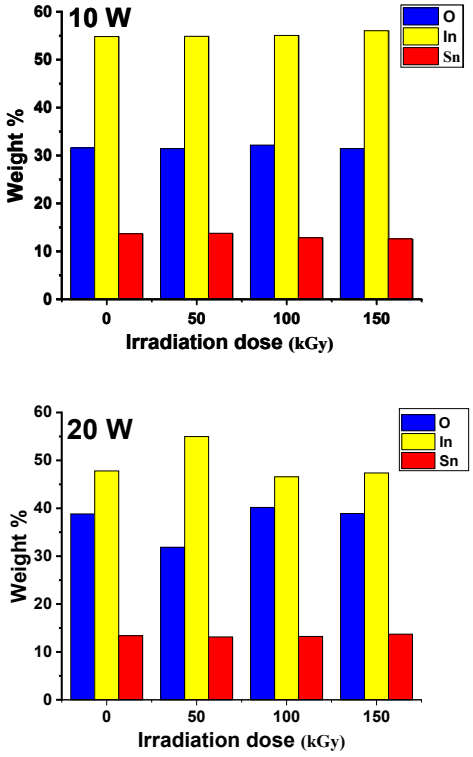

Figure 4. EDS results of ITO films comparing the concentrations of O, In, and Sn at different irradiation doses

3.3 Optical studies

The optical transmittance spectra of the ITO films after gamma irradiation showed a significant decrease in transmittance as radiation intensity increased, as illustrated in Figure 5. This phenomenon is caused by high-energy gamma photons interacting with the ITO film and glass, causing changes within the structure. As a result, increased structural defects and irregularities in the crystal lattice occur. These defects primarily arise from trapping electrons and ions excited by high-energy radiation, leading to increased light scattering and absorption (Mustapha et al., 2018). Furthermore, the damage induced by irradiation may alter the electronic energy levels within the film, affecting its optical properties and reducing its efficiency in applications requiring high transmittance. Consequently, the ITO film becomes progressively opaque as the radiation dose increases.

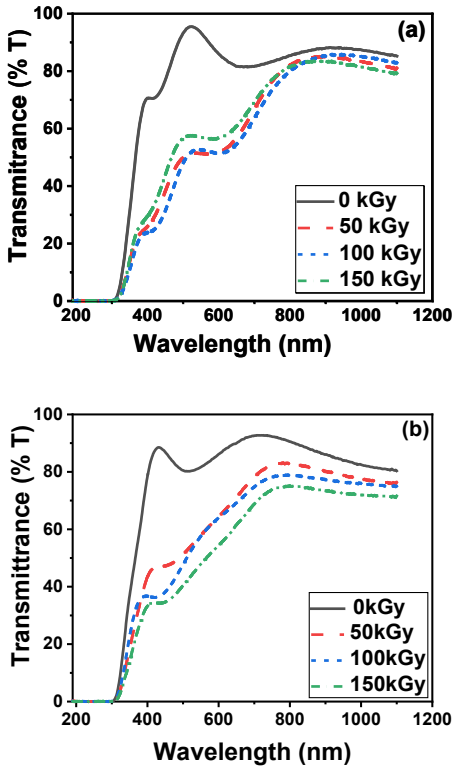

Figure 5. Optical transmission spectra of glass/ITO films deposited with sputtering powers of 10 and 20 W at varying gamma radiation doses

Figure 6 shows the energy gap (E_g) of gamma-irradiated and unirradiated ITO films calculated using the Tauc plot method (Kakil et al., 2018). For the unirradiated film, the E_g was around 3.69 eV. This value was close to that of commercial ITO, which exhibited a band gap in the range of 3.5-4.3 eV (University Wafer, Inc.). It is noted that the band gap is influenced by the film thickness and the fabrication method (Mukhokosi et al., 2017; Pawar et al., 2018). However, after gamma irradiation of 150 kGy, the E_g decreased to 3.53 eV for the film deposited with a power of 20 W and from 3.69 eV to 3.55 eV for the power of 10 W. The E_g values are shown in Table 2.

In terms of sputtering power, films deposited at 20 W exhibited larger grains and consequently a more pronounced bandgap narrowing compared to those deposited at 10 W. With increasing gamma dose (50-150 kGy), Eg progressively decreased, indicating defect accumulation and enhanced structural disorder.

This result also reflected a shift in the absorption edge toward longer wavelengths (red shift), which was consistent with bandgap narrowing due to defect accumulation. This result was consistent with the experimental results reported by Joseph and Balasundaram (2017), which showed a decrease in the light band as the radiation dose increased. This result can be explained by the change in crystallite size and the creation and destruction of structural defects induced by gamma irradiation (Deng et al., 1999). In addition, oxygen

deficiency may contribute under certain conditions, although EDS results suggested oxygen content remained relatively stable in the 10 W films.

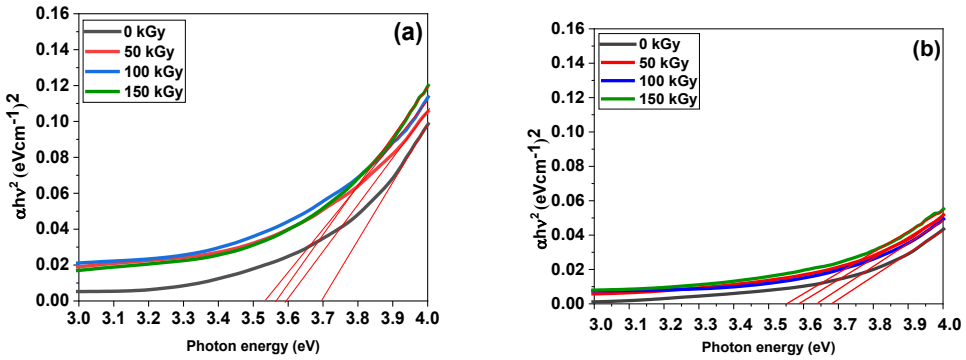

Figure 6. Energy gap of ITO films produced with sputtering powers of (a) 10 and (b) 20 W at varying gamma radiation doses

Table 2. Energy gap of gamma-unirradiated and irradiated ITO films

Sputtering Power	Gamma Dose (kGy)			
	0	50	100	150
10 W	3.694±0.016	3.594±0.013	3.532±0.019	3.565±0.005
20 W	3.691±0.005	3.637±0.016	3.584±0.023	3.550±0.011

In conclusion, higher sputtering power (20 W) results in larger grain size and greater bandgap narrowing, while increasing gamma dose (50-150 kGy) promoted defect generation, atomic rearrangement, and grain fragmentation, leading to a progressive decrease in E_g and modified optical performance.

3.4 Electrical properties

Table 3 presents the electrical properties of ITO films subjected to gamma radiation, measured using the Four-Point Probe technique. In terms of sputtering power, films deposited at 20 W initially exhibited higher crystallinity and moderate conductivity but were more sensitive to irradiation-induced degradation compared to 10 W films, which showed more gradual changes in resistivity. For films deposited at 10 W, conductivity decreased at 50 kGy and 100 kGy, followed by a slight increase at 150 kGy. In contrast, films deposited at 20 W exhibited an initial decrease in conductivity at 50 kGy, an increase at 100 kGy, and a subsequent decrease at 150 kGy. At 150 kGy, all irradiated films displayed lower conductivity than their unirradiated counterparts.

Regarding the effect of gamma irradiation dose, conductivity generally declined with increasing dose, consistent with increased resistivity. A temporary improvement at 50 kGy (in 20 W films) suggested partial radiation-induced recrystallization, whereas higher doses (≥100 kGy) caused defect accumulation and dominant carrier scattering. This can be explained by the change in electrical resistance. Before gamma irradiation, the ITO film exhibited a resistivity of 0.735×10^{-3} Ω·cm, which was greater than the resistivity of

commercial ITO-coated glass of 1.5 × 10^{-4} Ω·cm (XY15S, XINYAN TECHNOLOGY

Table 3. Resistivity values of ITO films under various conditions

Sample	Gamma Dose (kGy)	Electrical Properties		
		Resistivity (Ω·cm)	Carrier Mobility (cm^2/Vs)	Bulk Concentration (cm^{-3})
10 W	0	$0.735\times10^{-3}\pm0.001$	28.553 ± 0.026	$2.972\times10^{20}\pm0.024$
	50	$1.949\times10^{-3}\pm0.001$	20.463 ± 0.004	$1.564\times10^{20}\pm0.003$
	100	$2.235\times10^{-3}\pm0.001$	17.140 ± 0.004	$1.629\times10^{20}\pm0.004$
	150	$2.140\times10^{-3}\pm0.001$	18.953 ± 0.006	$1.539\times10^{20'}\pm0.006$
20 W	0	$0.943\times10^{-3}\pm0.001$	25.050 ± 0.006	$2.649\times10^{20}\pm0.007$
	50	$1.485\times10^{-3}\pm0.001$	20.920 ± 0.007	$2.007\times10^{20}\pm0.007$
	100	$1.110\times10^{-3}\pm0.001$	25.30 ± 0.007	$2.223\times10^{20}\pm0.006$
	150	$1.762\times10^{-3}\pm0.001$	21.73 ± 0.003	$1.630\times10^{20}\pm0.003$

LIMITED, Hong Kong). However, after irradiation, an increase in resistivity was observed, suggesting increased defect formation and structural degradation. These variations can be correlated with changes in crystallinity, carrier mobility, and bulk carrier concentration.

As shown in XRD analysis (Figure 2), increasing radiation dose reduced peak intensity and crystallite size, indicating structural disorder and defect accumulation. These defects disrupted charge transport by introducing additional grain boundaries and increasing carrier scattering, leading to decreased mobility, as observed in Table 3. At 50 kGy, ITO films deposited at 20 W exhibited an increase in crystallinity, as revealed by XRD, coinciding with a temporary conductivity improvement. This behavior suggests radiation-induced recrystallization, where moderate defect formation may have facilitated grain growth and improved carrier transport. However, at 100 kGy and 150 kGy, defect accumulation dominated, leading to a decline in crystallinity and increased grain boundary scattering, which suppressed carrier mobility and conductivity.

Additionally, bulk carrier concentration fluctuated with irradiation, likely due to defect-assisted carrier trapping and recombination. While oxygen vacancies can introduce free carriers and enhance conductivity, the EDS results (Figure 4) indicated that oxygen concentration remained relatively stable across different irradiation doses. This suggests that the observed changes in conductivity were primarily driven by microstructural damage (as seen in FE-SEM results, Figure 3), grain boundary modifications, and defect-induced carrier scattering rather than by oxygen vacancy formation alone.

Although films deposited at 20 W initially showed higher crystallinity and moderate conductivity, those deposited at 10 W demonstrated more consistent structural and electrical behavior under increasing irradiation doses. The relatively gradual change in resistivity and crystallinity at 10 W suggests that lower sputtering power may lead to enhanced radiation tolerance. Although not conclusive, these results may indicate that films deposited at lower sputtering power exhibit reduced sensitivity to radiation-induced structural and electrical degradation. Further studies are needed to validate this trend.

The contrasting behavior observed between the 10 W and 20 W sputtered ITO films can be attributed to differences in deposition energy and resulting film microstructure.

Higher sputtering power (20 W) typically leads to increased adatom energy, which enhances surface mobility and promotes crystallinity. However, it may also induce internal stress and denser microstructure, making the films more susceptible to defect generation and carrier scattering under gamma irradiation. In contrast, the 10 W films, although initially more disordered, may possess lower internal stress and exhibit more gradual changes in resistivity and bandgap, indicating a potentially higher tolerance to radiation-induced degradation. These results suggest that deposition parameters play a critical role in determining the radiation response of ITO films, not only through initial crystallinity but also via the balance between film density, defect dynamics, and structural relaxation during irradiation.

Overall, sputtering power determines the initial crystallinity and conductivity (20 W > 10 W), whereas gamma irradiation dose governs the extent of degradation: moderate doses (50 kGy) can temporarily enhance conductivity through recrystallization, but higher doses (≥100 kGy) consistently reduce mobility and increase resistivity.

4. Conclusions

This study analyzed the effects of gamma radiation on the structural, optical, and electrical properties of ITO films prepared by DC magnetron sputtering at different sputtering powers. It was found that irradiation reduced crystallinity, increased defect formation, and led to potential amorphization at high radiation doses (≥100 kGy). These structural changes resulted in decreased light transmittance, reduced energy gap, and lowered electrical conductivity, indicating increased resistivity due to defect accumulation. EDS analysis showed a particularly stable oxygen composition at a power of 10 W, indicating that the main cause of these changes was due to atomic rearrangement and formation of radiation-induced defects rather than oxygen loss. Variations in carrier mobility and concentration indicated that defect-assisted carrier scattering and recombination play significant roles in altering electrical transport properties. These changes were critical to understanding and improving ITO films for radiation-exposed environments

5. Acknowledgements

The authors would like to extend their sincere thanks to the Department of Physics, Faculty of Science and Technology, Thammasat University, the Division of Physics, Faculty of Science and Technology, Rajamangala University of Technology Thanyaburi, the National Electronics and Computer Technology Center (NECTEC) and the National Institute of Nuclear Technology for providing the necessary experimental facilities.

6. Authors' Contributions

Nalutporn Phiboon prepared film, conducted measurement, analyzed results, and wrote the manuscript; Watcharaporn Thongjoon contributed new reagents/analytic tools; Chantana Aiempanakit performed research; Akapong Phunpueok contributed new reagents/analytic tools, analyzed data; Sarawut Jaiyen contributed new reagents/analytic tools, analyzed data; Montri Aiempanakit wrote the manuscript; and Kamon Aiempanakit designed research, performed research.

ORCID

Nalutporn Phiboon https://orcid.org/0009-0006-0015-6306

Kamon Aiempanakit https://orcid.org/0000-0002-5709-5528
Montri Aiempanakit https://orcid.org/ 0000-0003-3162-0790
Chantana Aiempanakit https://orcid.org/0000-0002-5709-5528
Akapong Phunpueok https://orcid.org/0000-0002-9745-3457

7. Conflicts of Interest

The authors declare no conflict of interest.

References

Aiempanakit, K., Rakkwamsuk, P., & Dumrongrattana, S. (2009). Influence of continuous and discontinuous depositions on properties of ITO films prepared by DC magnetron sputtering. *Modern Physics Letters B*, *23*(26), 3157-3170. https://doi.org/10.1142/s0217984909021211

Al-Baradi, A. M., El-Nahass, M. M., El-Raheem, M. M. A., Atta, A. A., & Hassanien, A. M. (2014). Effect of gamma irradiation on structural and optical properties of Cd_2SnO_4 thin films deposited by DC sputtering technique. *Radiation Physics and Chemistry, 103*, 227-233. https://doi.org/10.1016/j.radphyschem.2014.05.055

Aldawood, S., & Ali, S. M. (2024). Effects of gamma irradiation on the properties of Ce_2S_3 thin films. *Journal of King Saud University - Science, 36*(2), Article 103075. https://doi.org/10.1016/j.jksus.2023.103075

Al-Hardan, N. H., Abdullah, M. J., & Aziz, A. A. (2013). Performance of Cr-doped ZnO for acetone sensing. *Applied Surface Science, 270*, 480-485. https://doi.org/10.1016/j.apsusc.2013.01.064

Alyamani, A., & Mustapha, N. (2016). Effects of high dose gamma irradiation on ITO thin film properties. *Thin Solid Films, 611*, 27-32. https://doi.org/10.1016/j.tsf.2016.05.022

Chauhan, R. N., Anand, R. S., & Kumar, J. (2014). RF-sputtered Al-doped ZnO thin films: Optoelectrical properties and application in photovoltaic devices. *Physica Status Solidi (a), 211*(11), 2514-2522. https://doi.org/10.1002/pssa.201431107

Comini, E., Baratto, C., Concina, I., Faglia, G., Falasconi, M., Ferroni, M., Galstyan, V., Gobbi, E., Ponzoni, A., Vomiero, A., Zappa, D., Sberveglieri, V., & Sberveglieri, G. (2013). Metal oxide nanoscience and nanotechnology for chemical sensors. *Sensors and Actuators B: Chemical, 179*, 3-20. https://doi.org/10.1016/j.snb.2012.10.027

Coutts, T. J., Young, D. L., Li, X., Mulligan, W. P., & Wu, X. (2000). Search for improved transparent conducting oxides: A fundamental investigation of CdO, Cd_2SnO_4, and Zn_2SnO_4. *Journal of Vacuum Science & Technology A: Vacuum, Surfaces, and Films, 18*(6), 2646-2660. https://doi.org/10.1116/1.1290371

Deng, Q., Yin, Z., & Zhu, R. (1999). Radiation-induced color centers in La-doped $PbWO_4$ crystals. *Nuclear Instruments and Methods in Physics Research Section A: Accelerators, Spectrometers, Detectors and Associated Equipment, 438*(2-3), 415-420. https://doi.org/10.1016/s0168-9002(99)00835-9

Diliegros-Godines, C. J., Flores-Ruiz, F. J., Castanedo-Pérez, R., Torres-Delgado, G., Espinoza-Beltrán, F. J., & Broitman, E. (2014). Mechanical and tribological properties of CdO + SnO_2 thin films prepared by sol–gel. *Journal of Sol-Gel Science and Technology, 74*(1), 114-120. https://doi.org/10.1007/s10971-014-3584-1

El-Nahass, M. M., Atta, A. A., El-Shazly, E. A. A., Faidah, A. S., & Hendi, A. A. (2009). Influence of γ-irradiation on the optical properties of nanocrystalline tin phthalocyanine thin films. *Materials Chemistry and Physics, 117*(2-3), 390-394. https://doi.org/10.1016/j.matchemphys.2009.06.015

El-Nahass, M. M., El-Deeb, A. F., Metwally, H. S., El-Sayed, H. E. A., & Hassanien, A. M. (2010). Influence of X-ray irradiation on the optical properties of iron (III) chloride tetraphenylporphyrin thin films. *Solid State Sciences, 12*(4), 552-557. https://doi.org/10.1016/j.solidstatesciences.2010.01.004

Joseph, S., & Balasundaram, O. N. (2017). Effect of gamma radiation on structural, optical and electrical properties of ZnO thin films. *Optoelectronics and Advanced Materials – Rapid Communications, 11*(5-6), 377-380.

Kajal, R., Kataria, B. R., Asokan, K., & Mohan, D. (2023). Effects of gamma radiation on structural, optical, and electrical properties of SnO_2 thin films. *Applied Surface Science Advances, 15*, Article 100406. https://doi.org/10.1016/j.apsadv.2023.100406

Kakil, S. A., Sabr, B. N., Hana, L. S., Abbas, T. A.-H., & Hussin, S. Y. (2018). Effects of a low dose of gamma radiation on the morphology, and the optical and the electrical properties of an ITO thin film as an electrode for solar cell applications. *Journal of the Korean Physical Society, 72*(5), 561-569.

Khodorov, A., Piechowiak, M., & Gomes, M. J. M. (2007). Structural, electrical and optical properties of indium–tin–oxide thin films prepared by pulsed laser deposition. *Thin Solid Films*, *515*(20-21), 7829-7833. https://doi.org/10.1016/j.tsf.2007.04.017

Kim, S. I., Lee, K. W., Sahu, B. B., & Han, J. G. (2015). Flexible OLED fabrication with ITO thin film on polymer substrate. *Japanese Journal of Applied Physics, 54*(9), Article 090301. https://doi.org/10.7567/jjap.54.090301

Kulkarni, A. K., Schulz, K. H., Lim, T.-S., & Khan, M. (1997). Electrical, optical and structural characteristics of indium-tin-oxide thin films deposited on glass and polymer substrates. *Thin Solid Films, 308-309*, 1-7. https://doi.org/10.1016/s0040-6090(97)00526-9

Kumaravel, R., Gokulakrishnan, V., Ramamurthi, K., Sulania, I., Kanjilal, D., Asokan, K., & Avasthi, D. K. (2010). Effect of swift heavy ion irradiation on structural, optical and electrical properties of Cd_2SnO_4 thin films. *Nuclear Instruments and Methods in Physics Research Section B: Beam Interactions with Materials and Atoms, 268*(15), 2391-2394. https://doi.org/10.1016/j.nimb.2010.04.029

Li, X., Gessert, T. A., & Coutts, T. (2004). The properties of cadmium tin oxide thin-film compounds prepared by linear combinatorial synthesis. *Applied Surface Science, 223*(1-3), 138-143. https://doi.org/10.1016/s0169-4332(03)00909-7

Maknys, K., Ulyashin, A. G., Stiebig, H., Kuznetsov, A. Yu., & Svensson, B. G. (2006). Analysis of ITO thin layers and interfaces in heterojunction solar cells structures by AFM, SCM and SSRM methods. *Thin Solid Films, 511-512*, 98-102. https://doi.org/10.1016/j.tsf.2005.12.006

Mukhokosi, E. P., Krupanidhi, S. B., & Nanda, K. K. (2017). Band gap engineering of hexagonal $SnSe_2$ nanostructured thin films for infra-red photodetection. *Scientific Reports*, *7*(1), Article 15215. https://doi.org/10.1038/s41598-017-15519-x

Mustapha, N., Alkaoud, A., Alyamani, A., & Idriss, H. (2018). Influence of gamma ray onto transparent indium tin oxide thin films. *Journal of Ovonic Research*, *14*(3), 225-233.

Mustapha, N., Ibnaouf, K. H., Fekkai, Z., Hennache, A., Prasad, S., & Alyamani, A. (2013). Improved efficiency of solar cells based on BEHP-co-MEH-PPV doped with ZnO nanoparticles. *Optik, 124*(22), 5524-5527. https://doi.org/10.1016/j.ijleo.2013.03.161

Oryema, B., Jurua, E., Madiba, I. G., Nkosi, M., Sackey, J., & Maaza, M. (2020). Effects of low-dose γ-irradiation on the structural, morphological, and optical properties of fluorine-doped tin oxide thin films. *Radiation Physics and Chemistry, 176*, Article 109077. https://doi.org/10.1016/j.radphyschem.2020.109077

Pawar, V., Jha, P. K., Panda, S. K., Jha, P. A., & Singh, P. (2018). Band-gap engineering in ZnO thin films: A combined experimental and theoretical study. *Physical Review Applied*, *9*(5), Article 054001. https://doi.org/10.1103/physrevapplied.9.054001

Rossnagel, S. (2001). Sputtering and sputter deposition. In R. F. Bunshah (Ed.). *Handbook of hard coatings: Deposition technologies, properties and applications* (pp. 319-348). Elsevier. https://doi.org/10.1016/B978-081551442-8.50013-4

Tahar, R. B. H., Ban, T., Ohya, Y., & Takahashi, Y. (2001). Effect of processing parameters on physical properties of cadmium stannate thin films prepared by a dip-coating technique. *Journal of the American Ceramic Society, 84*(1), 85-91. https://doi.org/10.1111/j.1151-2916.2001.tb00612.x

Venkatachalam, S., Nanjo, H., Kawasaki, K., Hayashi, H., Ebina, T., & Mangalaraj, D. (2011). *Optoelectronic properties of ZnSe, ITO, TiO_2 and ZnO thin films*. InTech. https://doi.org/10.5772/18418

Wohlmuth, W., & Adesida, I. (2005). Properties of R.F. magnetron sputtered cadmium–tin–oxide and indium–tin–oxide thin films. *Thin Solid Films*, *479*(1-2), 223-231. https://doi.org/10.1016/j.tsf.2004.11.186

Wu, X., Mulligan, W. P., & Coutts, T. J. (1996). Recent developments in RF sputtered cadmium stannate films. *Thin Solid Films, 286*(1-2), 274-276. https://doi.org/10.1016/s0040-6090(95)08527-0

Yan, M., Lane, M., Kannewurf, C. R., & Chang, R. P. H. (2001). Highly conductive epitaxial CdO thin films prepared by pulsed laser deposition. *Applied Physics Letters*, *78*(16), 2342-2344. https://doi.org/10.1063/1.1365410